

# Structural Variation in Novel Double Salts of Silver Acetylide with Silver Nitrate: Fully Encapsulated Acetylide Dianion in Different Polyhedral Silver Cages<sup>†</sup>

Guo-Cong Guo,<sup>‡</sup> Gong-Du Zhou,<sup>§</sup> and Thomas C. W. Mak<sup>\*,‡</sup>

Contribution from the Department of Chemistry, The Chinese University of Hong Kong, Shatin, New Territories, Hong Kong

Received November 30, 1998

**Abstract:** The reaction of silver acetylide with silver nitrate at 80 °C yielded a mixture of the known compounds  $\text{Ag}_2\text{C}_2 \cdot 6\text{AgNO}_3$  (**1**) and  $\text{Ag}_2\text{C}_2 \cdot 5.5\text{AgNO}_3 \cdot 0.5\text{H}_2\text{O}$  (**2**), which have different crystal habits and could be manually separated.  $\text{Ag}_2\text{C}_2 \cdot 5\text{AgNO}_3$  (**3**) was obtained serendipitously as a mixed product together with **1** from the addition of  $\text{AgNO}_3$  to a solution of the double salt of  $\text{Ag}_2\text{C}_2$  with  $\text{CF}_3\text{COOAg}$  at 80 °C.  $\text{Ag}_2\text{C}_2 \cdot \text{AgNO}_3$  (**4**) was obtained by carrying out a hydrothermal reaction at 105 °C. Complexes **2** and **3** contain a monocapped octahedral silver cage and a monocapped trigonal prismatic silver cage, respectively, each fully entrapping an acetylide dianion. In complex **4**, silver octahedra each encapsulating an acetylide dianion are connected by linking their equatorial edges along the *a* and *b* directions to form a slab, and the sharing of apexes between adjacent slabs along the *c* direction then generates a three-dimensional network. The bonding interaction between the acetylide dianion, which exhibits triple-bond character, and the cage silver atoms in complexes **1–4** is of the mixed  $\sigma, \pi$ -type, except that with a few silver atoms mainly  $\sigma$  bonding or  $\pi$  bonding can be clearly recognized. The different structural alternatives adopted by this series of related complexes suggests that a higher molar composition of silver acetylide in a double salt favors the formation of a network of edge- and vertex-sharing silver polyhedra that approaches the unknown crystal structure of silver acetylide.

## Introduction

Acetylene is a Brønsted acid, and the acetylide monoanion  $\text{HC}\equiv\text{C}^-$  and its substituted derivatives have a rich organometallic chemistry.<sup>1</sup> On the other hand, much less is known about the ligand behavior of the acetylide dianion,  $\text{C}_2^{2-}$ . Acetylides of the groups 1, 2, 11, and 12 metals have been known for some considerable time.<sup>2</sup> Many alkaline-earth and lanthanide carbides  $\text{MC}_2$  adopt the tetragonal  $\text{CaC}_2$  (I) structure,<sup>3</sup> which consists of a packing of  $\text{Ca}^{2+}$  and discrete  $\text{C}_2^{2-}$  ions in a distorted NaCl

lattice with the  $\text{C}_2^{2-}$  moieties (bond length 1.191 Å from neutron powder diffraction<sup>4</sup>) aligned parallel to the *c* axis.<sup>5</sup> There is no detailed structural information on the alkali-metal acetylides  $\text{M}_2\text{C}_2$ , except that the crystal structure of  $\text{Li}_2\text{C}_2$ <sup>6</sup> resembles that of  $\text{CaC}_2$  (I). The group 11 ( $\text{Cu}_2\text{C}_2$ ,  $\text{Ag}_2\text{C}_2$ , and  $\text{Au}_2\text{C}_2$ ) and group 12 ( $\text{ZnC}_2$ ,  $\text{CdC}_2$ ,  $\text{Hg}_2\text{C}_2 \cdot \text{H}_2\text{O}$ , and  $\text{HgC}_2$ ) acetylides exhibit properties that are characteristic of covalent polymeric solids, but their proneness to detonation upon mechanical shock and insolubility in common solvents present serious difficulties in structural characterization.

\* To whom correspondence should be addressed. Tel.: (852) 2609-6279. Fax: (852) 2603-5057. E-mail: tcwmak@cuhk.edu.hk.

<sup>†</sup> Dedicated to Professor Charles A. McDowell on the occasion of his 80th birthday.

<sup>‡</sup> The Chinese University of Hong Kong.

<sup>§</sup> On sabbatical leave from Department of Chemistry, Peking University, Beijing, P. R. China.

(1) For latest papers and reviews, see: (a) Goldfuss, B.; Schleyer, P. v. R.; Hampel, F. *J. Am. Chem. Soc.* **1997**, *119*, 1072. (b) Yam, V. W.-W.; Fung, W. K.-M.; Cheung, K.-K. *Organometallics* **1997**, *16*, 2032. (c) Brasse, C.; Raithby, P. R.; Rennie, M.-A.; Russell, C. A.; Steiner, A.; Wright, D. S. *Organometallics* **1996**, *15*, 639. (d) Ara, I.; Berenger, J. R.; Forniés, J.; Lalinde, E.; Moreno, M. T. *J. Organomet. Chem.* **1996**, *510*, 63. (e) Diederich, F.; Faust, R.; Gramlich, V.; Seiler, P. *J. Chem. Soc., Chem. Commun.* **1994**, 2045. (f) Lang, H.; Kohler, K.; Blau, S. *Coord. Chem. Rev.* **1995**, *143*, 113. (g) Decker, S. A.; Klobukowski, M. *J. Am. Chem. Soc.* **1998**, *120*, 9342. (h) Okazaki, M.; Ohtani, T.; Inomata, Tagaki, N.; Ogino, H. *J. Am. Chem. Soc.* **1998**, *120*, 9135. (i) Miguel, D.; Moreno, M.; Perez, J.; Riera, V.; Churchill, D. G.; Churchill, M. R.; Janik, T. S. *J. Am. Chem. Soc.* **1998**, *120*, 417.

(2) (a) Frad, W. F. *Adv. Inorg. Chem. Radiochem.* **1968**, *11*, 153. (b) Thompson, N. R. In *Comprehensive Inorganic Chemistry*; Bailar, J. C. Jr., Emeléus, H. J., Nyholm, R., Trotman-Dickenson, A. F., Eds.; Pergamon Press: Oxford, 1973; Vol. 3, p 102.

(3) (a) Wells, A. F. *Structural Inorganic Chemistry*, 5th ed.; Clarendon Press: Oxford, 1984; p 948. (b) Mak, T. C. W.; Zhou, G.-D. *Crystallography in Modern Chemistry: A Resource Book of Crystal Structures*; Wiley-Interscience: New York, 1992; p 285.

The earliest known<sup>7</sup> and most studied nonionic acetylide is  $\text{Ag}_2\text{C}_2$ , which forms a series of double salts of the general formula  $\text{Ag}_2\text{C}_2 \cdot m\text{AgX}$ , where  $\text{X}^- = \text{Cl}^-$ ,  $\text{I}^-$ ,  $\text{NO}_3^-$ ,  $\text{H}_2\text{AsO}_4^-$ , or  $1/2\text{EO}_4^{2-}$  (E = S, Se, Cr, or W) and *m* is the molar ratio.<sup>8</sup> Of the reported double salts  $\text{Ag}_2\text{C}_2 \cdot m\text{AgNO}_3$  (*m* = 1, 2, 6),  $\text{Ag}_2\text{C}_2 \cdot 6\text{AgNO}_3$  (**1**) was initially characterized by X-ray crystallography with the acetylide dianion wrongly positioned in the unit cell,<sup>9a</sup> and in the revised crystal structure the acetylide dianion was shown to be disordered about a crystallographic 3-fold axis that bisects the  $\text{C}\equiv\text{C}$  bond and passes through two opposite corners of an elongated  $\text{Ag}_8$  rhombohedron.<sup>9b</sup> The acetylide dianion is thus fully encapsulated inside a rhombohedral silver cage, and this situation can be conveniently represented as  $[\text{C}_2@\text{Ag}_8]$  (Figure 1E). Two other double salts of silver acetylide,  $\text{Ag}_2\text{C}_2 \cdot$

(4) (a) Atoji, M.; Medrud, R. C. *J. Chem. Phys.* **1959**, *31*, 332. (b) Atoji, M. *J. Chem. Phys.* **1961**, *35*, 1950.

(5) Ruiz, E.; Alemany, P. *J. Phys. Chem.* **1995**, *99*, 3114.

(6) Juza, R.; Wehle, V. *Naturwissenschaften* **1965**, *52*, 537.

(7) (a) Quet, J. A. C. R. *Hebd. Seances Acad. Sci.* **1858**, *46*, 903. (b) Bertholet, M. P. C. R. *Hebd. Seances Acad. Sci.* **1860**, *50*, 805.

(8) Vestin, R.; Ralf, E. *Acta Chem. Scand.* **1949**, *3*, 101.

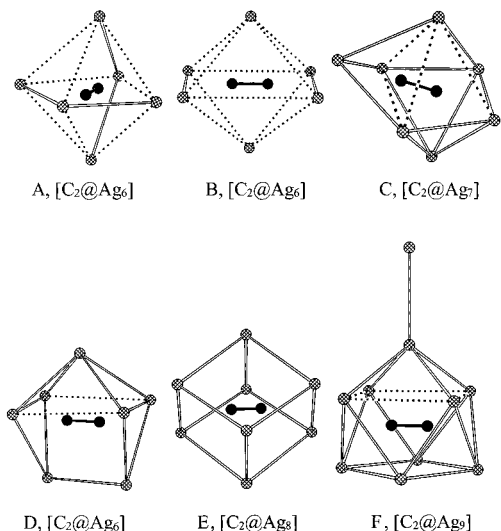


**Figure 1.** Silver cages that fully encapsulate the  $C_2^{2-}$  dianion in double salts of silver acetylide. Polyhedral edges that are longer than 3.40 Å (twice the van der Waals radius of the silver atom) are represented by dotted lines.

$8AgF^{10}$  and  $Ag_2C_2 \cdot 2AgClO_4 \cdot 2H_2O$ ,<sup>11</sup> were recently synthesized in our laboratory and shown to contain square antiprismatic  $[C_2@Ag_8-Ag]$  (Figure 1F) and octahedral  $[C_2@Ag_6]$  assemblies (Figure 1A), respectively. In the latter structure, the encapsulated  $C_2^{2-}$  ion is  $\sigma$ -bonded to two vertexes and  $\pi$ -bonded to four vertexes of the  $Ag_6$  octahedron. We herein report the synthesis and crystal structures of three new "lower molar ratio" double salts of silver acetylide with silver nitrate, namely  $Ag_2C_2 \cdot 5.5AgNO_3 \cdot 0.5H_2O$  (**2**),  $Ag_2C_2 \cdot 5AgNO_3$  (**3**), and  $Ag_2C_2 \cdot AgNO_3$  (**4**), in which the acetylide dianion is located inside a silver cage having the shape of a monocapped octahedron (Figure 1C), a monocapped trigonal prism (Figure 1D), and an octahedron (Figure 1B), respectively. Refinement of the crystal structure of **1** using a new data set is included here for ready reference and comparison.

## Experimental Section

All starting materials were purchased from the Aldrich Chemical Co.

**Synthesis of  $Ag_2C_2$ .** Aqueous silver nitrate solution was stirred, and a slow stream of acetylene gas was bubbled into it until saturation was reached at ambient temperature. The white precipitate of  $Ag_2C_2$  was isolated by filtration, washed several times with deionized water, and stored in the dark in the wet state. **CAUTION:** thoroughly dried  $Ag_2C_2$  detonates easily upon mechanical shock, and only a small quantity should be prepared for immediate use in any chemical reaction.

**Synthesis of  $Ag_2C_2 \cdot 5.5AgNO_3 \cdot 0.5H_2O$ , **2**.** About 1.0 g of moist  $Ag_2C_2$  was added to 2 mL of distilled water. The white slurry was stirred at 80 °C, and  $AgNO_3$  was added stepwise until the solid material was completely dissolved. The solution was placed in a desiccator filled with  $P_2O_5$ . After several days a good crop of mixed crystals of **1** (rhombohedral blocks, estimated yield 30%) and **2** (plates, estimated yield 15%) was deposited, which could be separated manually as they have different habits. **CAUTION:** violent decomposition occurs when the double salts of silver acetylide with silver nitrate are heated.

**Synthesis of  $Ag_2C_2 \cdot 5AgNO_3$ , **3**.** This complex was obtained unexpectedly from an attempt to prepare the double salt of  $Ag_2C_2$  with  $CF_3COOAg$ . Moist  $Ag_2C_2$  was added to 2 mL of a concentrated aqueous solution of  $CF_3COOAg$ , with stirring, at 80 °C until saturation was reached. The excess amount of  $Ag_2C_2$  was filtered off, and the solution was placed in a desiccator charged with  $P_2O_5$ . Complete evaporation yielded a gluey residue, which was redissolved in distilled water and a small amount of solid  $AgNO_3$  was added with stirring at 80 °C. The resulting solution was kept at 0 °C for several days, after which a mixture of crystals of **1** (estimated yield 15%) and **3** (estimated yield 10%) was deposited. Prismatic crystals of **3** can be clearly distinguished and picked out from among the blocklike crystals of **1**.

**Synthesis of  $Ag_2C_2 \cdot AgNO_3$ , **4**.** This complex was synthesized using the hydrothermal technique as described in our previous papers.<sup>12</sup> Moist  $Ag_2C_2$  was added to 4 mL of a concentrated aqueous solution of  $AgNO_3$  (about 40%) under stirring until saturation occurred. The excess amount of  $Ag_2C_2$  was filtered off, and the filtrate was transferred into a glass tube. The tube was sealed and put into an autoclave under a nitrogen atmosphere, slowly heated to 105 °C for 48 h, and then slowly cooled to 80 °C at 6 °C/h. The same reaction was also performed by replacing distilled water with ethanol. Colorless prismatic crystals of **4** (estimated yield 30%) can be easily isolated in each case.

The Raman spectra (Renishaw Raman Image Microscope System 2000) of **2** and **3** exhibit twin absorption peaks in the  $\Delta\nu(C\equiv C)$  region at (2103.8, 2167.0) and (2103.8, 2166.9)  $cm^{-1}$ , respectively, which originate from Fermi resonance between the stretching frequency of  $C_2^{2-}$  and the first overtone of the irradiating laser line at 1123.4  $cm^{-1}$ . The Raman spectra of **1** and **4**, measured in an altered setting to avoid the irradiating laser line, exhibit single  $\Delta\nu(C\equiv C)$  absorption peaks at 2083 and 2069  $cm^{-1}$ , respectively.

**X-ray Crystallographic Studies.** Colorless crystals mounted inside 0.3-mm Lindemann glass capillaries were used for data collection on a Rigaku RAXIS IIC imaging plate diffractometer for **1**, **3**, and **4** and on a Rigaku AFC7R diffractometer for **2** using graphite-monochromated Mo K $\alpha$  radiation ( $\lambda = 0.71073$  Å) from a rotating-anode generator powered at 50 kV and 90 mA. For **2**, the data set was collected out to  $2\theta = 60^\circ$  using the  $\omega$ -scan technique and corrected for absorption (relative transmission factors 0.839–1.0) on the basis of  $\psi$ -scan, yielding 5272 reflections (5180 independent,  $R_{int} = 0.0512$ ). For **1**, **3**, and **4**, 20, 46, and 26 oscillation frames were taken in the range of  $\phi = 0-180^\circ$  with  $\Delta\phi = 7.2, 3.5,$  and  $6.0^\circ$ , and 10-, 10-, and 8-min exposure per frame, respectively. The data sets of **1**, **3**, and **4** were corrected using ABSCOR<sup>13</sup> with relative transmission factors in the range 0.842–1.0, 0.779–1.0, and 0.548–1.0, yielding 1604 (597 independent,  $R_{int} = 0.0787$ ), 3973 (1395 independent,  $R_{int} = 0.0699$ ), and 860 (150 independent,  $R_{int} = 0.0742$ ) reflections, respectively. The unit-cell parameters of **4** were in good agreement with the results obtained from powder diffraction.<sup>14</sup> All structures were solved by direct methods (SHELXS-86) and refined by full-matrix least squares on  $F^2$  using the Siemens SHELXTL-93 (PC Version) package of crystallographic software.<sup>15</sup> Crystallographic data and refinement parameters are listed in Table 1, and selected bond distances and angles are given in Table 2.

The atom Ag(8) in **2** is located on a crystallographic 2-fold axis and is not bonded to the other silver atoms, and one of the six independent nitrate anions (composed of atoms N(6), O(16), O(17), and O(18)) has 1/2 site occupancy. All non-hydrogen atoms were refined anisotropically except for O(16) and water oxygen atoms O(1W) and O(1W'), which have 1/4 site occupancy in **2**. The silver atoms in **3** exhibit unusually large thermal parameters, and the capping atom was found to be disordered about two sites (represented by Ag(4) and

(9) (a) Österlöf, J. *Acta Crystallogr.* **1954**, *7*, 637. (b) Jin, X.-L.; Zhou, G.-D.; Wu, N.-Z.; Tang, Y.-Q.; Huang, H.-C. *Acta Chem. Sin. (Chin. Ed.)* **1990**, *48*, 232. A description of the structure is given in: Mak, T. C. W.; Zhou, G.-D. *Crystallography in Modern Chemistry: a Resource Book of Crystal Structures*; Wiley-Interscience: New York, 1992; p 288.

(10) Guo, G.-C.; Zhou, G.-D.; Wang, Q.-G.; Mak, T. C. W. *Angew. Chem., Int. Ed. Engl.* **1998**, *37*, 630.

(11) Guo, G.-C.; Wang, Q.-G.; Zhou, G.-D.; Mak, T. C. W. *J. Chem. Soc., Chem. Commun.* **1998**, 339.

(12) (a) Guo, G.-C.; Kwok, R. W. M.; Mak, T. C. W. *Inorg. Chem.* **1997**, *36*, 2475. (b) Guo, G.-C.; Mak, T. C. W. *J. Chem. Soc., Dalton Trans.* **1997**, 709. (c) Guo, G.-C.; Mak, T. C. W. *Inorg. Chem.* **1998**, *37*, 6538.

(13) Higashi, T. ABSCOR – An Empirical Absorption Correction Based on Fourier Coefficient Fitting, Rigaku Corporation, Tokyo, (c) 1995.

(14) Redhouse, A. D. Woodward, P. *Acta Crystallogr.* **1964**, *17*, 616.

(15) (a) Sheldrick, G. M. in *Crystallographic Computing 6: A Window on Modern Crystallography*; Flack, H. D., Párkányi, L., Simon, K., Eds.; Oxford University Press: Oxford, 1993; p 111. (b) SHELXTL/PC version 5 Reference Manual, Siemens Energy & Automation, Inc., Madison, WI, 1996.

**Table 1.** Crystallographic Data and Structure Refinement Parameters

	1	2	3	4
chemical formula	Ag <sub>2</sub> C <sub>2</sub> ·6AgNO <sub>3</sub>	Ag <sub>2</sub> C <sub>2</sub> ·5.5AgNO <sub>3</sub> ·0.5H <sub>2</sub> O	Ag <sub>2</sub> C <sub>2</sub> ·5AgNO <sub>3</sub>	Ag <sub>2</sub> C <sub>2</sub> ·AgNO <sub>3</sub>
formula weight	1259.04	1183.11	1089.16	409.64
space group	R $\bar{3}$ (No. 148)	C2/c (No. 15)	I $\bar{4}2d$ (No. 122)	I4/mmm (No. 139)
<i>a</i> , Å	7.935(1)	28.539(2)	12.001(2)	7.336(2)
<i>b</i> , Å	7.935(1)	8.043(1)	90	90
<i>c</i> , Å	7.935(1)	15.825(1)	22.030(4)	9.416(3)
$\beta$ , deg	106.05(1)	102.21(1)	90	90
<i>V</i> , Å <sup>3</sup>	426.41(9)	3550.3(6)	3172.8(9)	506.7(3)
<i>Z</i>	1	8	8	4
$\rho_{\text{calcd}}$ , g cm <sup>-3</sup>	4.903	4.427	4.560	5.369
<i>T</i> , °C	293(2)	293(2)	293(2)	293(2)
$\lambda$ , Å	0.710 73	0.710 73	0.710 73	0.710 73
$\mu$ , cm <sup>-1</sup>	91.00	81.99	85.55	113.83
<i>R</i> <sup>a</sup>	0.0595	0.0532	0.0868	0.0407
<i>Rw</i> <sup>b</sup>	0.1436	0.1181	0.2688	0.1043

<sup>a</sup>  $R = \sum(|F_o| - |F_c|) / \sum|F_o|$ . <sup>b</sup>  $R_w = \sum w(F_o^2 - F_c^2)^2 / \sum w(F_o^2)^2$ .  $w^{-1} = [\sigma^2(F_o)^2 + (aP)^2 + bP]$  where  $P = (F_o^2 + 2F_c^2)/3$ , and  $(a, b) = (0.0634, 5.3025)$ ,  $(0.0595, 0)$ ,  $(0.1605, 0)$ , and  $(0, 11.5045)$ , respectively.

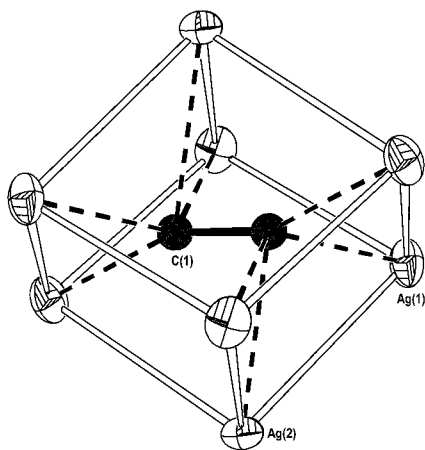


**Figure 2.** Perspective drawing of the rhombohedral [C<sub>2</sub>@Ag<sub>8</sub>] assembly in Ag<sub>2</sub>C<sub>2</sub>·6AgNO<sub>3</sub>, **1**. The silver cage has symmetry  $\bar{3}$ , and the disordered acetylide dianion is shown in one of its three possible orientations. The thermal ellipsoids are drawn at the 30% probability level.

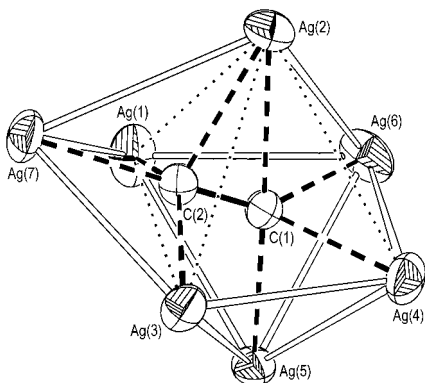


**Figure 3.** Perspective drawing of the capped octahedral [C<sub>2</sub>@Ag<sub>7</sub>] assembly in Ag<sub>2</sub>C<sub>2</sub>·5.5AgNO<sub>3</sub>·0.5H<sub>2</sub>O, **2**. Note that the C<sub>2</sub><sup>2-</sup> unit is directed toward the capping atom Ag(7). The thermal ellipsoids are drawn at the 30% probability level. The dotted lines represent the lengthened Ag...Ag distances (longer than 3.40 Å).

Ag(4A), each having half-site occupancy) that are related by symmetry 2 and are 1.064 Å apart. Another data set was recollected using a different crystal of **3**, but virtually the same structural analysis results were obtained. For **4**, the Laue symmetry is 4/mmm, and the space group was chosen as I4/mmm in preference to other alternatives. The nitrogen atom of the nitrate anion in **4** occupies a site of symmetry 4mm and the oxygen atoms are accordingly disordered. In the model adopted for refinement, the oxygen atoms were assigned the same

isotropic thermal parameter, and the sum of their site occupancy factors was fixed at 12/32 = 0.375. The maximum and minimum residual peaks in **1–4** all occur in the vicinity of the Ag atoms.

## Results and Discussion

Compound **1** can be easily prepared by dissolving Ag<sub>2</sub>C<sub>2</sub> in a concentrated aqueous solution of AgNO<sub>3</sub> at room temperature. Above the concentration threshold of Ag<sup>+</sup> ions, the concentration and solvents used do not affect the result. The reaction temperature employed seems to be important for the preparation of double salts with a higher molar composition of Ag<sub>2</sub>C<sub>2</sub>. At 80 °C, **2** together with **1** were obtained. However, no other phase was detected up to reflux condition. The hydrothermal technique, which was successfully employed in preparing metal polychalcogenides,<sup>12</sup> yielded crystals of **4** at 105 °C using either distilled water or ethanol as solvent. It is worthy of note that the previously reported synthetic route to **4** only gave a powdery product.<sup>14</sup> Crystals of **3** turned out to be a windfall from an attempt to prepare the double salt of Ag<sub>2</sub>C<sub>2</sub> with CF<sub>3</sub>COOAg, which was not obtained by variation of the reaction conditions such as the concentration of CF<sub>3</sub>COOAg, temperature, solvent, or hydrothermal synthesis. The rationale for adding AgNO<sub>3</sub> into the solution of CF<sub>3</sub>COOAg and Ag<sub>2</sub>C<sub>2</sub> was that doing so could promote the threshold concentration of Ag<sup>+</sup> ions required for dissolution of Ag<sub>2</sub>C<sub>2</sub>. The role played by CF<sub>3</sub>COOAg in the formation of a double salt with higher molar composition of Ag<sub>2</sub>C<sub>2</sub> is not clear, and further explorations are in progress.

Our improved data set for **1** is consistent with the reported structural model,<sup>9b</sup> in which the acetylide dianion is located within a rhombohedral Ag<sub>8</sub> cage with a crystallographic 3-fold axis bisecting the C=C bond and passing through two opposite vertices (Figure 2). The Ag...Ag and Ag–C distances range from 2.9546(5) to 3.0521(6) and 2.089(9) to 2.488(8) Å, respectively. The Ag<sub>7</sub> cage in **2** is best described as a monocapped octahedron with four lengthened edges, in which the acetylide dianion is fully encapsulated and directed toward the capping atom Ag(7), with the atoms C(1) and C(2) lying 0.196 and 0.586 Å above the Ag(1)–Ag(3)–Ag(4)–Ag(6) plane, respectively (Figure 3). The Ag...Ag distances in the resulting [C<sub>2</sub>@Ag<sub>7</sub>] assembly range from 2.9073(5) to 3.3604(5) Å, which are shorter than twice the van der Waals radius of silver (2 × 1.70 Å), suggesting that weak Ag...Ag interactions may exist. The Ag<sub>7</sub> cage that accommodates the acetylide dianion in **3** has crystallographically imposed symmetry 2; it can be described as a monocapped trigonal prism with lengthening of two opposite edges of its expanded capped face, and the capping

**Table 2.** Selected Bond Lengths (Å) and Angles (deg) for **1-4**

Compound 1			
Ag(1)–Ag(1) <sup>a</sup>	2.9546(5)	C(1)–Ag(1) <sup>b</sup>	2.346(12)
Ag(1)–Ag(2)	3.0521(6)	C(1)–Ag(2) <sup>c</sup>	2.488(8)
C(1)–Ag(1) <sup>d</sup>	2.480(14)	C(1)–C(1) <sup>e</sup>	1.22(2)
Ag(1)–C(1)	2.089(9)		
C(1) <sup>c</sup> –C(1)–Ag(1) <sup>d</sup>	99.7(14)	C(1) <sup>c</sup> –C(1)–Ag(1) <sup>b</sup>	113.8(13)
C(1) <sup>c</sup> –C(1)–Ag(1)	154.1(7)	C(1) <sup>c</sup> –C(1)–Ag(2) <sup>c</sup>	78.3(7)
Compound 2			
Ag(1)–Ag(5)	3.3545(5)	Ag(1)–C(2)	2.277(3)
Ag(1)–Ag(6)	3.1774(6)	Ag(2)–C(2)	2.347(3)
Ag(1)–Ag(7)	3.0379(5)	Ag(3)–C(2)	2.362(3)
Ag(2)–Ag(6)	3.1908(6)	Ag(4)–C(1)	2.167(3)
Ag(2)–Ag(7)	3.3604(5)	Ag(5)–C(1)	2.332(3)
Ag(3)–Ag(4)	3.0502(5)	Ag(6)–C(1)	2.193(3)
Ag(3)–Ag(5)	3.3412(5)	Ag(7)–C(2)	2.108(3)
Ag(3)–Ag(7)	3.1677(4)	C(1)–C(2)	1.180(4)
Ag(4)–Ag(5)	2.9619(5)	Ag(8)–O(1) <sup>d</sup>	2.411(2)
Ag(4)–Ag(6)	2.9073(5)	Ag(8)–O(1)	2.411(2)
Ag(5)–Ag(6)	3.2213(5)	Ag(8)–O(5) <sup>d</sup>	2.428(2)
Ag(2)–C(1)	2.437(3)	Ag(8)–O(5)	2.428(2)
C(2)–C(1)–Ag(2)	71.5(2)	Ag(5)–C(1)–Ag(2)	175.2(2)
C(2)–C(1)–Ag(4)	142.2(3)	Ag(6)–C(1)–Ag(2)	86.96(10)
C(2)–C(1)–Ag(5)	107.1(2)	Ag(1)–C(2)–Ag(2)	105.07(11)
C(2)–C(1)–Ag(6)	131.4(3)	Ag(2)–C(2)–Ag(3)	107.56(13)
C(1)–C(2)–Ag(1)	96.3(2)	Ag(7)–C(2)–Ag(2)	97.77(11)
C(1)–C(2)–Ag(2)	80.0(2)	O(1) <sup>d</sup> –Ag(8)–O(1)	85.06(12)
C(1)–C(2)–Ag(3)	87.3(2)	O(1) <sup>d</sup> –Ag(8)–O(5) <sup>d</sup>	119.94(9)
C(1)–C(2)–Ag(7)	175.9(3)	O(1)–Ag(8)–O(5) <sup>d</sup>	121.82(8)
Ag(4)–C(1)–Ag(2)	101.70(13)	O(1) <sup>d</sup> –Ag(8)–O(5)	121.82(8)
Ag(4)–C(1)–Ag(5)	82.25(10)	O(1)–Ag(8)–O(5)	119.94(9)
Ag(4)–C(1)–Ag(6)	83.64(12)	O(5) <sup>d</sup> –Ag(8)–O(5)	91.72(11)
Compound 3			
Ag(1)–Ag(1) <sup>e</sup>	3.106(2)	Ag(3)–Ag(4) <sup>e</sup>	2.712(2)
Ag(1)–Ag(2)	2.9225(12)	Ag(1)–C(1)	2.257(6)
Ag(1)–Ag(3)	3.1353(15)	Ag(2)–C(1)	2.051(5)
Ag(2)–Ag(3)	3.033(2)	Ag(3)–C(1)	2.098(5)
Ag(2)–Ag(4)	2.846(2)	Ag(4)–C(1)	2.416(6)
Ag(2)–Ag(4) <sup>e</sup>	3.232(2)	Ag(4)–C(1) <sup>e</sup>	2.401(6)
Ag(3)–Ag(4)	3.361(2)	C(1)–C(1) <sup>e</sup>	1.224(10)
C(1) <sup>e</sup> –C(1)–Ag(1)	114.56(13)	Ag(2)–C(1)–Ag(4) <sup>e</sup>	92.8(2)
C(1) <sup>e</sup> –C(1)–Ag(2)	138.7(5)	Ag(3)–C(1)–Ag(4) <sup>e</sup>	73.8(2)
C(1) <sup>e</sup> –C(1)–Ag(3)	119.5(6)	Ag(1)–C(1)–Ag(4) <sup>e</sup>	165.6(2)
C(1) <sup>e</sup> –C(1)–Ag(4)	74.6(2)	Ag(2)–C(1)–Ag(4)	78.7(2)
C(1) <sup>e</sup> –C(1)–Ag(4) <sup>e</sup>	76.0(2)	Ag(3)–C(1)–Ag(4)	96.0(2)
Ag(2)–C(1)–Ag(3)	94.0(2)	Ag(1)–C(1)–Ag(4)	162.5(3)
Ag(2)–C(1)–Ag(1)	85.3(2)	Ag(4) <sup>e</sup> –C(1)–Ag(4)	25.51(10)
Ag(3)–C(1)–Ag(1)	92.0(2)		
Compound 4			
Ag(1)–Ag(1) <sup>f</sup>	2.9253(9)	Ag(2)–C(1)	2.432(1)
Ag(1)–C(1)	2.163(3)	C(1)–C(1) <sup>h</sup>	1.225(7)
C(1) <sup>h</sup> –C(1)–Ag(1)	137.44(6)	Ag(1)–C(1)–Ag(2)	100.69(5)
C(1) <sup>h</sup> –C(1)–Ag(2)	75.42(8)	Ag(2)–C(1)–Ag(2) <sup>h</sup>	150.8(2)
Ag(1) <sup>g</sup> –C(1)–Ag(1)	85.1(1)		

<sup>a</sup>  $-z + 1, -x + 1, -y + 1$ . <sup>b</sup>  $-y + 1, -z + 1, -x + 1$ . <sup>c</sup>  $-x + 1, -y + 1, -z + 1$ . <sup>d</sup>  $-x + 1, y, -z + 3/2$ . <sup>e</sup>  $-x + 1, -y + 1, z$ . <sup>f</sup>  $y, -x, -z$ . <sup>g</sup>  $-y, x, z$ . <sup>h</sup>  $-x, -y + 1, -z$ .

atom (represented by Ag(4) and Ag(4A) in Figure 4) is asymmetrically positioned owing to 2-fold disorder about the 2 axis. The Ag⋯Ag distances of the [C<sub>2</sub>@Ag<sub>7</sub>] assembly in **3** range from 2.712(2) to 3.361(2) Å, being also suggestive of the existence of weak Ag⋯Ag interactions. In either **2** or **3**, the shortest Ag⋯Ag distance is comparable to the interatomic contact of 2.89 Å in silver metal and, hence, indicative of interactions of the same order of magnitude. The crystal structures of **1**, **2**, and **3** are all three-dimensional frameworks, in which the nitrate anions serve as bridges between adjacent polyhedra with Ag–O distances ranging from 2.381(2) to 1.467(2), 2.178(4) to 2.588(5), and 2.204(4) to 2.553(6) Å, respectively.

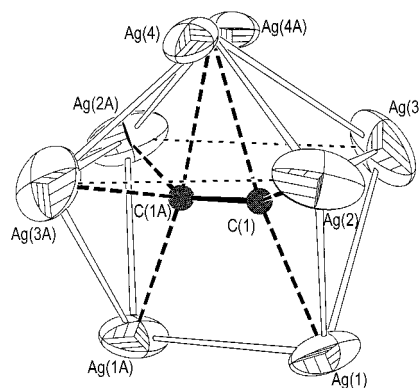


**Figure 4.** Perspective drawing of the capped trigonal prismatic [C<sub>2</sub>@Ag<sub>7</sub>] assembly in Ag<sub>2</sub>C<sub>2</sub>·5AgNO<sub>3</sub>, **3**. The silver cage has symmetry 2, and the capping atom is disordered over two sites as represented by Ag(4) and Ag(4A). The thermal ellipsoids are drawn at the 30% probability level. The dotted lines represent the lengthened Ag⋯Ag distances (longer than 3.40 Å).

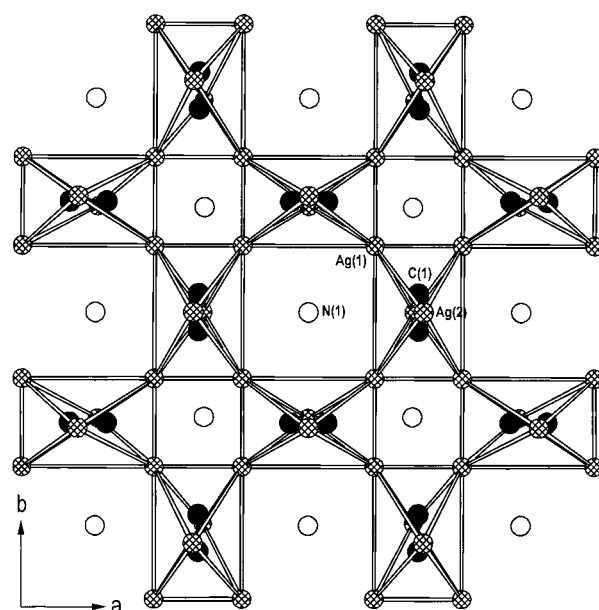


**Figure 5.** Slab formed by the linkage of [C<sub>2</sub>@Ag<sub>6</sub>] assemblies in Ag<sub>2</sub>C<sub>2</sub>·AgNO<sub>3</sub>, **4**, viewed along the *c* direction. For clarity, the nitrate anions are represented as circles, and the Ag–C bonds are omitted.

In contrast to **1**, **2**, and **3**, in which the silver polyhedra are discrete and interlinked by NO<sub>3</sub><sup>−</sup> anions, the silver octahedra in **4** are connected in the *a* and *b* directions to form a slab (Figure 5), and sharing of the remaining apices in such slabs along the *c* direction leads to a three-dimensional cationic network (Figure 6). The disordered NO<sub>3</sub><sup>−</sup> anions are located in square channels generated from the linkage of silver octahedra (Figure 5). In comparison with the silver octahedron in Ag<sub>2</sub>C<sub>2</sub>·2AgClO<sub>4</sub>·2H<sub>2</sub>O, in which the C<sub>2</sub><sup>2−</sup> species lies along a diagonal of the equatorial plane (Figure 1A), the C<sub>2</sub><sup>2−</sup> species in **4** lies parallel to the pair of longer sides in the equatorial plane of the encapsulating octahedron (Figure 1B).

Figure 1 shows the versatile coordination modes of the C<sub>2</sub><sup>2−</sup> dianion fully encapsulated inside different silver polyhedra. The thick broken lines in Figures 2, 3, 4, and 6 represent bonding interactions between the acetylide dianion and the cage silver atoms in **1**, **2**, **3**, and **4**, respectively. In **2**, the coordination mode of the acetylide dianion to atoms Ag(7) and Ag(2) can be regarded as *σ*-bonding (Ag(7)–C(2) 2.108(3) Å, Ag(7)–C(2)–C(1) 175.9(3)°) and side-on *π*-bonding (Ag(2)–C(1) 2.437(3),

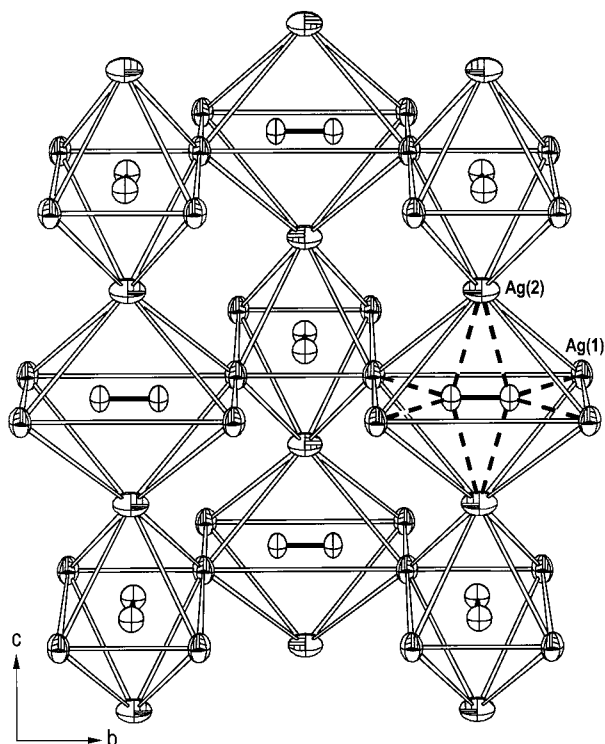


**Figure 6.** Stack of slabs in  $\text{Ag}_2\text{C}_2\cdot\text{AgNO}_3$ , **4**, viewed along the  $c$  direction. For clarity, the Ag–C bonds (thick broken lines) are shown only for one of the encapsulated  $\text{C}_2^{2-}$  anions.

$\text{Ag}(2)\text{--C}(2)$  2.347(3) Å, respectively (Figure 3). Similar types of bonding interaction have been observed in  $[\text{Cu}_4(\mu\text{-dppm})_4(\mu_4\text{-}\eta^1, \eta^2\text{-C}_2)](\text{BF}_4)_2$ <sup>16</sup> and  $\text{Ag}_2\text{C}_2\cdot 2\text{AgClO}_4\cdot 2\text{H}_2\text{O}$  (see Figure 1A),<sup>11</sup> in which the bonding of the acetylide dianion to  $\text{Cu}^{\text{I}}$  and  $\text{Ag}^{\text{I}}$  centers shows a clear distinction between  $\sigma$  and  $\pi$  coordination modes. However, the bonding interaction between the acetylide dianion and the other five cage silver atoms in **2** is ambiguous, with Ag–C bond distances of 2.167(3) to 2.362(3) Å and C–C–Ag bond angles ranging from 87.3(2) to 142.2(3)°. As shown in Figure 4, analogous mixed  $\sigma$ ,  $\pi$ -bonding interaction also occurs in **3** between the acetylide dianion and the cage silver atoms (Ag–C distances ranging from 2.051(5) to 2.416(6) Å; C(1A)–C(1)–Ag angles ranging from 114.6(1) to 138.7(5)°) except for the capping atom, which binds the acetylide dianion in the side-on  $\pi$ -bonding mode (Ag(4)–C(1) 2.416(6), Ag(4)–C(1A) 2.401(6) Å). Similarly, in both the rhombohedral  $[\text{C}_2@\text{Ag}_8]$  assembly of **1** and the monocapped square antiprismatic  $[\text{C}_2@\text{Ag}_8\text{-Ag}]$  assembly of  $\text{Ag}_2\text{C}_2\cdot 8\text{AgF}$ , the bonding interactions between the acetylide dianion and all cage silver atoms are of the mixed  $\sigma$ ,  $\pi$  type.

Interestingly, the  $\text{C}_2^{2-}$  anion in **4** exhibits a novel coordination mode in which it is symmetrically  $\pi$ -bonded to a pair of “axial” Ag2 atoms, and the sp lone pair of each carbon atom overlaps with the empty 5s orbitals of a pair of “equatorial” Ag1 atoms (Figure 6). The C–C–Ag1 bond angle is 137.44(6)°. The side-on  $\pi$ -bonded Ag–C distance in **4** (2.432(1) Å) is comparable with those found in **2** and **3**, but the “bent  $\sigma$ -bonded” Ag–C distance in **4** (2.163(3) Å) is significantly longer than those involving linear  $\sigma$  bonding in **2** (2.108(3) Å) and  $\text{Ag}_2\text{C}_2\cdot 2\text{AgClO}_4\cdot 2\text{H}_2\text{O}$  (2.087(3) and 2.108(6) Å). The coordination mode of  $\text{C}_2^{2-}$  in **4** implies weakening of the  $\text{C}\equiv\text{C}$  triple bond as a consequence of metal-to-ligand back  $\pi$  bonding, similar to

the case found in silver complexes of alkynes.<sup>17</sup> The Raman spectrum also shows a red shift of  $\Delta\nu(\text{C}\equiv\text{C})$  in **4**.

Diverse types of transition-metal compounds containing a discrete  $\text{C}_2$  unit include (i) bimetallic  $\mu$ -ethynediyl systems such as  $\text{Cp}(\text{CO})_2\text{Ru--C}\equiv\text{C--Ru}(\text{CO})_2\text{Cp}$  and  $(\text{CO})_5\text{Re--C}\equiv\text{C--Re}(\text{CO})_5$ ;<sup>18</sup> (ii) transition metal dicarbido clusters such as  $[\text{PPN}][\text{Fe}_3(\text{CO})_9(\text{C}_2)\text{Re}(\text{CO})_5]$ ;<sup>19</sup> (iii) lanthanide halide dicarbido cluster complexes such as  $\text{Cs}_3[\text{Tb}_{10}(\text{C}_2)_2]\text{I}_{21}$ <sup>20</sup> and  $[\text{Er}_{14}(\text{C}_2)_2(\text{N}_2)_2]\text{I}_{24}$ ,<sup>21</sup> and (iv) solid-state ternary-metal dicarbides containing the  $\text{C}_2$  unit, a transition metal (Cr to Ni and their heavier congeners), and a highly electropositive multivalent metal (lanthanide, Sc, Y, or Th), such as  $\text{DyCoC}_2$  or  $\beta\text{-ScCrC}_2$ .<sup>22</sup> The observed C–C bond lengths of the  $\text{C}_2$  unit in the dicarbido clusters are generally significantly longer than that found in acetylene (1.205 Å).<sup>23</sup> Most ternary-metal dicarbides containing a discrete  $\text{C}_2$  unit have C–C bond distances in the range 1.32 to 1.47 Å, a lone exception being 1.60 Å in  $\beta\text{-ScCrC}_2$ ;<sup>24</sup> such  $\text{C}_2$  units can be regarded as  $\text{C}_2^{4-}$  and  $\text{C}_2^{6-}$ , which are derived from complete deprotonation of ethylene and ethane, respectively. In contrast, the measured  $\text{C}\equiv\text{C}$  bond distances of the acetylide dianion in **1**, **2**, **3**, and **4** are 1.22(2), 1.180(4), 1.22(1), and 1.225(7) Å, respectively, which are comparable to that found in acetylene. Therefore, the acetylide dianion in **1–4** retains the essential triple-bond character inherited from its parent silver acetylide, as in the case of  $\text{Ag}_2\text{C}_2\cdot 8\text{AgF}$ <sup>10</sup> (1.175(7) Å) and  $\text{Ag}_2\text{C}_2\cdot 2\text{AgClO}_4\cdot 2\text{H}_2\text{O}$ <sup>11</sup> (1.212(7) Å). The Raman spectra of **2** and **3** exhibit twin absorption peaks in the  $\Delta\nu(\text{C}\equiv\text{C})$  region at (2103.8, 2167.0) and (2103.8, 2166.9)  $\text{cm}^{-1}$ , respectively, which originate from Fermi resonance between the stretching frequency of  $\text{C}_2^{2-}$  and the first overtone of the irradiating laser line at 1123.4  $\text{cm}^{-1}$ . The Raman spectrum of **4** shows a redshift of  $\Delta\nu(\text{C}\equiv\text{C})$  to 2069  $\text{cm}^{-1}$  in comparison with **1** (2083  $\text{cm}^{-1}$ ), **2**, **3**,  $\text{Ag}_2\text{C}_2\cdot 8\text{AgF}$  (2104.5, 2168.6  $\text{cm}^{-1}$ ), and  $\text{Ag}_2\text{C}_2\cdot 2\text{AgClO}_4\cdot 2\text{H}_2\text{O}$  (2103.9, 2167.1  $\text{cm}^{-1}$ ).

Bond-valence calculation<sup>25</sup> on **1**, **2**, **3**, and **4** yielded average values of 0.874, 0.835, 0.978, and 0.877, respectively, for the nitrate anion, which are in reasonable agreement with its formal  $-1$  oxidation state. The calculated bond valences of the  $\text{C}_2^{2-}$  anion in the respective cages in  $\text{Ag}_2\text{C}_2\cdot 8\text{AgF}$  (3.086),  $\text{Ag}_2\text{C}_2\cdot 6\text{AgNO}_3$  (2.988),  $\text{Ag}_2\text{C}_2\cdot 5.5\text{AgNO}_3\cdot 0.5\text{H}_2\text{O}$  (3.346),  $\text{Ag}_2\text{C}_2\cdot 5\text{AgNO}_3$  (3.422), and  $\text{Ag}_2\text{C}_2\cdot \text{AgNO}_3$  (2.836) are all much larger

(17) (a) Brasse, C.; Raithby, P. R.; Rennie, M.-A.; Russell, C. A.; Steiner, A.; Wright, D. S. *Organometallics* **1996**, *15*, 639. (b) Yam, V. W.-W.; Fung, W. K.-M.; Cheung, K.-K. *Organometallics* **1997**, *16*, 2032. (c) Chi, K.-M.; Lin, C.-T.; Peng, S.-M.; Lee, G.-H. *Organometallics* **1996**, *15*, 2660.

(18) (a) Koutsantonis, G. A.; Selegue, J. P. *J. Am. Chem. Soc.* **1991**, *113*, 2316. (b) Heidrich, J.; Steimann, M.; Appel, M.; Beck, W.; Phillips, J. R.; Troglor, W. C. *Organometallics* **1990**, *9*, 1296. (c) Woodworth, B. E.; White, P. S.; Templeton, J. L. *J. Am. Chem. Soc.* **1998**, *120*, 9028, and references therein.

(19) Norton, D. M.; Eveland, R. W.; Hutchison, J. C.; Stern, C.; Shriver, D. F. *Organometallics* **1996**, *15*, 3916.

(20) Artelt, H. M.; Meyer, G. Z. *Anorg. Allg. Chem.* **1994**, *620*, 1527.

(21) Steffen, F.; Meyer, G. Z. *Naturforsch., Teil B* **1995**, *50*, 1570.

(22) King, R. B. *J. Organomet. Chem.* **1997**, *536–537*, 7, and references therein.

(23) (a) Halet, J. F.; Mingos, D. M. P. *Organometallics* **1988**, *7*, 51. (b) Akita, M.; Morooka, Y. *Bull. Chem. Soc. Jpn.* **1995**, *68*, 420.

(24) Pöttgen, R.; Witte, A. M.; Jeitschko, W.; Ebel, T. *J. Solid State Chem.* **1995**, *119*, 324.

(25) The individual bond valences have been calculated using the relation  $s_i = \exp[(R_0 - R)/b]$ , where  $R_0$  is a constant dependent on the assumed valence state of the central ion,  $R$  is the measured bond distance, and  $b$  is a constant whose value is available for a wide range of bond types. The atomic valences associated with a particular ion are calculated from  $V = \sum s_i$ . The  $R_0$  values of Ag–C and Ag–O of 1.89 and 1.805 Å, respectively, and  $b = 0.37$ , are taken from refs (a) and (b). (a) Brese, N. E.; O’Keefe, M. *Acta Cryst.* **1991**, *B47*, 192. (b) O’Keefe, M.; Brese, N. E. *Acta Cryst.* **1992**, *B48*, 152. (c) Brown, I. D. *Chem. Soc. Rev.* **1978**, *7*, 359. (d) Brown, I. D. in *Structure and Bonding in Crystals*, Vol. II; O’Keefe, M., Navrotsky, A., Eds.; Academic Press: New York, 1981.

(16) Yam, V. W.-W.; Fung, W. K.-M.; Cheung, K.-K. *Angew. Chem., Int. Ed. Engl.* **1996**, *35*, 1100.

than its formal oxidation state of  $-2$ . This mismatch may be taken to imply that bonding between the encapsulated acetylide dianion and the cage silver atoms is much more complex than can be accounted for by a simple theoretical model.

Since acetylene, azide, and cyanide are the longest established nitrogenase substrates,<sup>26,28</sup> and  $C_2^{2-}$  has the same set of molecular orbitals as  $N_2$ , the coordination modes of these species are of interest in connection with the binding of  $N_2$  to the FeMo cofactor of nitrogenase, whose crystal structure has been determined at medium resolution.<sup>27,28</sup> Two structural models have been proposed for  $N_2$  binding and reduction at the nitrogenase metalcenter: (1) the substrate lies completely within an expanded cofactor cavity and is surrounded by six Fe atoms in a trigonal prismatic environment,<sup>29</sup> leading to destabilization of the  $N\equiv N$  triple bond; (2) the substrate binds externally to an  $Fe_4$  rhombus face of a twisted form of the central  $Fe_6$  trigonal prism,<sup>30</sup> which was inspired by computation on the metallocarbohedrene  $Ti_8C_{12}^+$ <sup>31</sup> in which each  $C_2^{2-}$  fragment is bound to a quadrilateral of metal atoms. In the former model the  $\mu_6$  coordination mode of  $N_2$ , denoted as  $N_2@Fe_6$ , is analogous to the  $N_3^-@Ag_6$  unit in  $AgN_3 \cdot 2AgNO_3$ <sup>32</sup> and also resembles the  $C_2^{2-}@Ag_n$  ( $n = 6, 7, 8, 9$ ) unit in the present

(26) (a) Schrauzer, G. N.; Kiefer, G. W.; Doemeny, P. A.; Kisch, H. *J. Am. Chem. Soc.* **1973**, *95*, 5582. (b) Newton, W. E.; Corbin, J. L.; Schneider, P. W.; Bulen, W. A. *J. Am. Chem. Soc.* **1971**, *93*, 268.

(27) Kim, J.; Rees, D. C. *Science* **1992**, *257*, 1677.

(28) Howard, J. B.; Rees, D. C. *Chem. Rev.* **1996**, *96*, 2965.

(29) (a) Chan, M. K.; Kim, J.; Rees, D. C. *Science (Washington, D.C.)* **1993**, *260*, 792; (b) Stavrev, K. K.; Zerner, M. C. *Chem—Eur. J.* **1996**, *2*, 83.

(30) (a) Dance, I. G. *Aust. J. Chem.* **1994**, *47*, 979. (b) Dance, I. G. *J. Chem. Soc., Chem. Commun.* **1998**, 523.

(31) (a) Guo, B. C.; Kerns, K. P.; Castleman, A. W., Jr. *Science* **1993**, *255*, 1411. (b) Guo, B. C.; Wei, S.; Purnell, J.; Buzza, S.; Castleman, A. W., Jr. *Science* **1992**, *256*, 515. (c) Wei, S.; Guo, B. C.; Purnell, J.; Buzza, S.; Castleman, A. W., Jr. *Science* **1992**, *256*, 818. (d) Reddy, B. V.; Khanna, S. N.; Jena, P. *Science* **1992**, *258*, 1640. (e) Pilgrim, J. S.; Duncan, M. A. *J. Am. Chem. Soc.* **1993**, *115*, 9724.

(32) Guo, G.-C.; Mak, T. C. W. *Angew. Chem., Int. Ed. Engl.* **1998**, *37*, 3268.

series of double salts of silver acetylide.<sup>9–11</sup> The fact that both  $N_3^-$  and  $C_2^{2-}$  exhibit strong tendencies to be engaged inside a polyhedral silver cage may provide some clue in understanding the binding and weakening of  $N_2$  in the FeMo cofactor cavity. As the metalcenter is located within a spongy protein environment and its two incomplete-cubane moieties are linked by flexible sulfur ligands, the central cavity may be envisaged to open up readily when an  $N_2$  molecule is “breathed” into it.

**Concluding Remarks.** We have shown that in the series of related double salts of silver acetylide, **1–4**, silver cages of different polyhedral geometries make their appearance, but the encapsulated acetylide dianion retains its essential triple-bond character, and mixed  $\sigma, \pi$ -bonding interaction between it and the cage silver atoms generally occurs. Judging from the newly available structural data, it appears that double salts with a high  $AgX: Ag_2C_2$  molar ratio,  $m$ , favor the formation of large discrete silver cages ( $Ag_n$  with  $n \geq 7$ ) which are, in turn, linked by anions X to generate a three-dimensional network; whereas those with low  $m$  tend to have small octahedral silver cages that share vertexes and edges, as in the case of the layer-type structure formed by vertex sharing in  $Ag_2C_2 \cdot 2AgClO_4 \cdot 2H_2O$ <sup>11</sup> and the three-dimensional structure derived from edge and vertex sharing in **4**. It is therefore envisaged that, as  $m$  approaches a small fraction, the structure of the double salt will closely resemble that of neat silver acetylide.

**Acknowledgment.** This work is supported by Direct Grant 2060129 of The Chinese University of Hong Kong and Hong Kong Research Grants Council Earmarked Grant Ref. No. CUHK 4022/98P.

**Supporting Information Available:** X-ray structural data including tables of atomic parameters, bond lengths and angles, and calculated bond valences for **1–4**. This material is available free of charge via the Internet at <http://pubs.acs.org>.

JA984117N